



Dove, C. A., Bradley, F. F. and Patwardhan, S. V. (2019) A material characterization and embodied energy study of novel clay-alginate composite aerogels. *Energy and Buildings*, 184, pp. 88-98.
(doi:[10.1016/j.enbuild.2018.10.045](https://doi.org/10.1016/j.enbuild.2018.10.045))

This is the author's final accepted version.

There may be differences between this version and the published version. You are advised to consult the publisher's version if you wish to cite from it.

<http://eprints.gla.ac.uk/175182/>

Deposited on: 13 December 2018

Enlighten – Research publications by members of the University of Glasgow
<http://eprints.gla.ac.uk>

1 A material characterisation and embodied energy study of novel 2 Clay-Alginate Composite Aerogels.

3
4 Cassandra A. Dove ^a, Fiona F. Bradley ^{b*}, Siddharth V. Patwardhan ^c

5
6 ^a Dept. of Architecture, University of Strathclyde, Glasgow, UK

7 ^b School of Engineering, University of Glasgow, Glasgow, UK

8 ^c Department of Chemical and Biological Engineering, University of Sheffield, UK

9 10 **ABSTRACT**

11 There is a growing incentive within the construction industry to design low energy buildings which
12 incorporate increased levels of insulation whilst also encouraging the use of 'green' materials which
13 have a low environmental impact and can contribute positively to sustainable building strategies.
14 Silica aerogels have received an increasing amount of attention in recent years as a contemporary
15 insulation material, but their wide-spread use is currently hindered by high costs and their high
16 embodied energy. This research project explores the development of a composite insulation material
17 proposed as an alternative to silica aerogel, which consists of natural components including clay and
18 a biopolymer obtained from seaweed known as alginate. Prototype specimens have been developed
19 and characterised in terms of their mechanical properties and microstructure allowing comparisons to
20 be made between five alginate types, each obtained from a different seaweed source. Whilst all of the
21 composites tested offered an improvement over the control sample, the results also demonstrated
22 that the type of alginate used has a significant influence on the compressive strength and modulus
23 values of the resulting composite materials. An analysis of the production process additionally
24 demonstrated that the freeze-drying element can have a significant impact on both the environment
25 and financial costs of producing such a material.

26 *Keywords: biopolymer; biocomposite; alginate; aerogel; clay; insulation*

28 1. INTRODUCTION

29 Since two thirds of the heat generated in a building can be lost through the building fabric (Carbon
30 Trust, 2012), the use of appropriate thermal insulation is critical in helping to minimise energy losses
31 and reduce fuel costs for the occupants. It also decreases the reliance on mechanical heating
32 systems. Effective insulation materials are generally those which have a cellular or porous structure, a
33 low density and a low thermal conductivity. Common products therefore include the likes of mineral
34 wool which typically achieves a thermal conductivity of 0.03 – 0.05 W/m-K (Cuce et al., 2014a).
35 Polymer based products such as polyurethane (PUR) and expanded polystyrene (EPS) are also
36 particularly good insulators, exhibiting thermal conductivities as low as 0.02 – 0.03 W/m-K (Jelle,
37 2011). However these petrochemical derived insulation materials also exhibit poor environmental
38 credentials due to energy-intensive processing techniques and the use of fluorocarbon gases
39 (Papadopoulos, 2005). Furthermore, PUR based products also perform poorly in fire scenarios and
40 can emit toxic substances such as hydrogen cyanide (Stec and Hull, 2011). When selecting insulation
41 materials, it is therefore important to consider both the environmental impacts associated with
42 production and the potential to reduce operational energy demand over the building's lifetime by
43 reducing heat loss (Lolli and Hestnes, 2014).

44 The use of natural, renewable materials has been identified as a potential means of reducing the
45 embodied energy and carbon footprint of buildings (Felton et al., 2013). Natural insulation products
46 which include organic fibres such as those obtained from plant or animal sources have been
47 commercialized in recent years and continue to be investigated with academic research (Korjenic et
48 al., 2011; Lopez Hurtado et al., 2016; Zach et al., 2016; Pedroso et al., 2017; Savio et al., 2018). The
49 thermal properties of these materials are typically within the 0.04 – 0.08 W/mK range (Sutton et al.,
50 2011; Schiavoni et al., 2016). This makes them generally inferior to polymer based products meaning
51 that greater thicknesses are required in order to achieve comparable thermal performance. Natural
52 materials are also disadvantaged in terms of their durability, moisture sensitivity and cost and
53 therefore form only a small part of the UK market (Sutton et al., 2011). On the other hand, LCA
54 studies (Schiavoni et al., 2016) have shown that the embodied energy and global warming potential
55 values of natural fibre products are generally lower than polymer based products, although some
56 natural products like cork can in fact be worse than the likes of EPS and PUR. Indeed, mineral wool

57 products also perform well in LCA terms despite being produced from non-renewable resources. As a
58 result, when selecting appropriate insulation materials, there is often a trade-off made between
59 technical performance, cost and environmental impact. Whilst mineral wool products remain the most
60 popular choice for standard building insulation (Kiss et al., 2013), offering the best balance between
61 cost and technical performance, alternatives which offer lower thermal conductivities are now being
62 investigated for high-performance applications. One such development is the introduction of aerogels
63 into the building insulation market. These materials originated from early research by Kistler (1932;
64 1934) and are prepared by removing the liquid phase from a hydrated gel using supercritical drying.
65 The result is a highly porous, low density material which can be formed into aerogel monoliths and
66 granules or combined with another material to form a composite product (Nosrati and Berardi, 2018).
67 The majority of commercially available aerogels are silica-based aerogels and these can be used as
68 high performance insulation products for buildings in the form of boards, blankets or loose-fill granules
69 (Jelle, 2011; Baetens et al., 2011;Thapliyal and Singh, 2014;Cuce et al., 2014a). They can also be
70 incorporated into vacuum insulation panels (VIPs), a composite product consisting of a cellular core
71 which is then vacuum sealed within a layer of foil faced plastic (Alam et al., 2011; Liang et al., 2017b).
72 More recent developments have included insulated plasters which incorporate silica aerogels (Stahl et
73 al., 2012; Buratti et al., 2017) and aerogel/glass fibre composites (UI Haq et al., 2017). Aerogel
74 products therefore offer very low thermal conductivities for relatively small thicknesses, making them
75 particularly useful within retrofit projects where space is often restricted (Martinez, 2017). For example
76 Lolli and Hestnes (2014) demonstrated that an aerogel insulation product of 45mm would achieve the
77 same thermal performance as 100mm of mineral wool. Furthermore, for a VIP, the equivalent
78 thickness was only 25mm. Indeed high performance VIPs with an aerogel core can reportedly
79 achieve thermal conductivities as low as 0.012 W/mK (Liang et al., 2017a) whilst Buratti et al. (2017)
80 described aerogel granules with a thermal conductivity of 0.019–0.023 W/(mK). Commercial silica
81 aerogel blankets offer values of 0.018 W/mK (Aspen Aerogels, 2011) but silica-based aerogels are
82 however disadvantaged with respect to their environmental performance due to the energy-intensive
83 production processes and hazardous solvents used in their production (Dowson et al., 2012). In
84 addition, high production costs are a limiting factor on their widespread use (Riffat and Qiu, 2013;
85 Cuce et al., 2014a), particularly in the case of monolithic aerogels which have been more difficult to
86 commercialize than granules and composite products (Nosrati and Berardi, 2018). Some authors

87 have therefore proposed alternatives to silica based aerogels which are derived from more
88 environmentally friendly precursors. Kistler (1932) for example experimented with various natural
89 substances such as cellulose, gelatine and agar during his early work and van Olphen (1967) also
90 studied various water-soluble polymers in combination with clay minerals. Aerogels produced from
91 other natural polymers such as starch (Druel et al., 2017) are also being investigated as a means of
92 producing thermal insulation materials. More recently, Schiraldi, Bandi & Gawryla (2006) have
93 developed a product known as Aeroclay™ using clay aerogels modified by a range of polymeric
94 substances: epoxy (Arndt et al., 2007); PVOH and various natural fibres (Finlay et al., 2007; Chen et
95 al., 2014); casein (Gawryla et al., 2008), natural rubber (Pojanavaraphan et al., 2010a) and alginate
96 (Chen et al., 2012). Reportedly, these clay-based composites can be manufactured at a competitive
97 price utilising a relatively simple freeze-drying process, making them potential alternatives to silica
98 aerogels (Dalton et al., 2010; Schiraldi et al., 2010). As discussed by (Madyan et al., 2016), the
99 physical properties of clay aerogels, including the density, thermal conductivity and combustion
100 behaviour, can also be tailored by modifying the processing conditions and through the use of various
101 additives or coatings. There are however limited details of the embodied energy of clay aerogels and
102 to what extent the inclusion of additives, whether synthetic or bio-based, influences their overall
103 environmental impact.

104 Given that the ideal product would be one which offers thermal properties comparable to high
105 performance insulations combined with minimal environmental impact, it was postulated by the
106 authors that a clay-polymer aerogel consisting of natural raw materials may offer a potential solution.
107 For the purposes of this study, a natural bentonite clay and one of the aforementioned biopolymers,
108 alginate, were therefore used to create a series of composite aerogel materials which could be
109 studied in relation to both their physical properties and production. Whilst a few studies have
110 demonstrated that aerogels with high porosity and low bulk density can be created using layered
111 silicates and alginate (Ohta and Nakazawa, 1995; Chen et al., 2012), the role of the alginate, which is
112 a biopolymer obtained from seaweed, is not discussed in great detail. This is an important aspect to
113 consider given that alginate is a natural material which can vary widely in its composition and
114 functionality depending of the specific seaweed from which it is sourced. There has therefore been no
115 comprehensive study to date which discusses the role of alginate variables (source, M/G ratio,
116 viscosity and concentration) on the structural properties of composite alginate-clay aerogels such as

117 density, mechanical strength and morphology. A total of four different alginate products were
118 therefore tested in order to assess the feasibility of producing such a composite and to determine the
119 relative importance of different alginate variables on the final properties of the aerogel. The final
120 objective was to assess both the commercial viability and environmental impact of the alginate-clay
121 composite in comparison with other aerogel materials.

122

123 **2. EXPERIMENTAL**

124 **2.1. Materials**

125 2.1.1. Alginate

126 Alginate is a biopolymer obtained from brown seaweeds - also referred to as macro-algae. More
127 specifically, alginate is the collective term for the salts of alginic acid which are obtained from the cell
128 walls of the macro-algae; these salts, usually in the form of sodium or potassium, contribute to 20-
129 60% of the algae's dry matter.(Rehm, 2009). Alginate is obtained by firstly washing the milled
130 seaweed in acid in order to eradicate the cross-linking ions and solubilize the alginate salts (McHugh,
131 2003). The resulting mixture is then filtered to separate the solid cell wall debris and cellulose residue
132 from the alginate solution. The aqueous sodium alginate is then dried and pulverised to produce a
133 sodium alginate powder. As a block co-polymer of (1-4)-linked β -D-mannuronic acid and α -L-
134 guluronic acid residues, alginate is often described in terms of its M/G ratio, relating to the proportions
135 of the M (mannuronic) and G (guluronic) units on the polymer chain. One of the most useful functional
136 properties of alginate is its gel-forming ability, particularly in the presence of multivalent cations such
137 as Ca^{2+} (Draget et al., 2006; Funami et al., 2009). Variables which are known to effect the gelation
138 mechanisms include the seaweed source, the molecular weight and the composition of the polymer
139 (Martinsen et al., 1989; Straatmann and Borchard, 2003). The ratio of the crosslinking ions (e.g. Ca^{2+})
140 to the carboxyl groups present on the alginate has also been shown to influence the gelation behavior
141 (Liu et al., 2003).

142 In this study four different alginate products were supplied by Marine Biopolymers Ltd. (Ayr, Scotland)
143 and obtained from seaweeds harvested from the west coast of Scotland. These were prototype
144 products which are currently under development and have not yet been commercialized. Two different

145 seaweed types were studied: the *Ascophyllum nodosum* (PR52) and the *Laminaria hyperborean*, the
 146 latter of which was separated into the stem (PR22 and PR24) and frond (PR32) components to
 147 provide additional compositional variables. A commercial alginate (AC) from Acros Organics was also
 148 used for comparison. The properties of all five alginate types used are summarised in TABLE 1. M/G
 149 ratios were provided by MBL and calculated using ¹H-NMR spectroscopy following existing methods
 150 (Grasdalen et al., 1979; Davis et al., 2003). Viscosity measurements were conducted using a
 151 Brookfield R/S Rheometer using 1 w/v% alginate solutions in 0.1 M NaCl at a temperature of 25°C.

152 TABLE 1: Alginate Properties

Specimen	Source	M/G Ratio	Intrinsic Viscosity (L/g)
AC	Commercial Alginate	0.83	0.63
PR22	L. hyperborea (stem*)	1.04	0.26
PR24	L. hyperborea (stem*)	0.23	0.48
PR32	L. hyperborea (frond**)	0.72	0.2
PR52	Ascophyllum Nodosum	0.77	0.2

153 *Stem = stalk-like component which forms structural backbone

154 **Frond = leaf-like components attached to stem

155

156 2.1.2. Clay

157 The clay used was a bentonite clay sourced from Acros Organics (Geel, Belgium). The pH of the clay
 158 was measured using a 1:5 volume ratio of dry clay to a 0.01 mol/L CaCl₂ solution (BS EN
 159 15933:2012). The liquid limit was calculated using the cone penetrometer method (BS 1377-2:1990)
 160 whilst the electrical conductivity was measured using a handheld conductivity meter. Cation exchange
 161 capacity and specific surface area were calculated from the Methylene Blue test (BS EN 933-9:2009)
 162 and the available calcium content was obtained by inductively coupled plasma (ICP) on a deionised
 163 water (DI) extract. The bentonite properties are summarised in TABLE 2.

164

165 TABLE 2: Bentonite Properties

pH	Liquid Limit (%)	Clay Mineralogy	Electrical Conductivity (µS/cm)	Cation Exchange Capacity (meq/100g)	Specific Surface Area (m ² /g)	Exchangeable Calcium (ppm)
8.6	76.7	Major: Montmorillonite, Quartz, Feldspar	1943	65	26	4,228

166

167

168 2.2. Specimen preparation

169 The clay-alginate aerogels in this study were prepared using methods similar to that of Schiraldi et al.
170 (2010) whereby separate 10 wt% solutions of the alginate and clay were prepared in DI water. These
171 were then mixed at a range of alg:clay ratios (A = 100:0, B = 75:25, C = 50:50, D = 25:75 and E =
172 0:100) and filled into in 2mL cryogenic vials. Flash freezing was conducted using iso-pentane and
173 liquid nitrogen followed by a minimum of 24 hours drying in a Scanvac CoolSafe 110-4 PRO 4lt freeze
174 dryer. The specimens were then removed from the dryer and stored in sealed vials until further
175 testing. The samples produced were cylinders of approximately 9mm diameter.

176 2.3. Characterisation

177 General observations were made regarding the quality and homogeneity of the final specimens. Each
178 aerogel monolith was also weighed and its dimensions measured using digital calipers. The unit mass
179 (g) and unit volume (cm³) were then used to calculate the bulk density (ρ). The mechanical strength of
180 the specimens was investigated based on the procedures outlined in BS EN 826:2013 and as
181 described in other similar studies (Nussinovitch et al., 1993; Chen et al., 2012; Martins et al., 2015).
182 Although compressive strength is not the most important property for insulating materials since these
183 materials are not typically load-bearing, they still require sufficient mechanical integrity to be handled.
184 Comparing the strength characteristics of the different compositions also gives an indication of which
185 combinations of the clay and alginate are most effective. Testing was conducted on the cylindrical
186 specimens which were cut using a scalpel to a height of ~15mm. The surfaces of the two parallel
187 faces were also gently sanded to create smooth surfaces. An INSTRON 5969 universal testing
188 machine was then used to apply a compressive force (F) to the material using a displacement rate of
189 5 mm/min. The compressive strength (σ_m) of the specimens was then calculated from the initial cross-
190 sectional area of the specimen (A_o) and the maximum force (F_m) at the yield point. Results were then
191 calculated as the mean value of three test samples calculated to the nearest 0.1 N/mm².

$$192 \quad \sigma_m = F_m / A_o \quad (1)$$

194 Compressive strain (\mathcal{E}) was calculated by dividing the change in specimen height (ΔH) by the original
195 height (H_o). The compression modulus of elasticity (E) was also calculated from the initial linear
196 gradient of the stress-stain plot, prior to the yield point.

197 Since the size, shape and volume of the pores have an important influence on the mechanical
198 strength, as well as transport properties such as and thermal conductivity and vapour permeability,
199 the internal morphology of the samples was also investigated. SEM analysis was initially performed
200 using a Field Emission (FE) microscope (HITACHI SU-6600) in order to generate magnified images of
201 the microstructure of the aerogel specimens. Thin sections of the material were cut from the monoliths
202 in order to expose the internal part of the aerogel and all samples were sputter coated in gold prior to
203 the analysis. Further investigation of the microstructure was also achieved by comparing the
204 porosities of the different samples. Common porosity measurement techniques such as Mercury
205 Intrusion Porisimetry (MIP) and N₂ adsorption are problematic for compressible materials since the
206 pressures exerted during measurement can transform the structure thereby leading to false pore
207 sizes (Scherer, 1998). In this case porosity was therefore estimated by calculating the theoretical
208 porosity of each sample using Equation 4, using the methods of Rassis et al. (2003), Longo et al.
209 (2013) and Wang et al. (2014), where ρ_b is the bulk density of the sample and ρ_p is the overall particle
210 density. The latter value was calculated based on the mass fraction of each component and particle
211 density estimates of 2.5 g/cm³ for bentonite (Kogel et al., 2006) and 1.59 for alginate (Aspinall, 2014).

$$P = \left(1 - \frac{\rho_b}{\rho_p}\right) \times 100\% \quad (2)$$

214 **2.4. Cost and Environmental Impacts**

215 In considering the commercial feasibility of using an alginate-clay aerogel as a building insulation
216 material, aspects such as cost and environmental impact were also investigated. Cost calculations
217 were performed based on data supplied by MBL but it should be noted that the costs were based on
218 lab-scale prototypes with a production volume of approximately 100 cm³. The calculations were also
219 based purely on the basic cost of consumables and the key production processes. Costs associated
220 with equipment, labour and overheads have not been included at this stage. Although advanced LCA
221 can be used to provide a detailed environmental profile for the whole-life cycle of a product, this would
222 require data which is not yet available. As a result only estimations of embodied energy and
223 embodied CO₂ were considered based on the quantities of materials used and the energy consumed
224 during the main production processes.

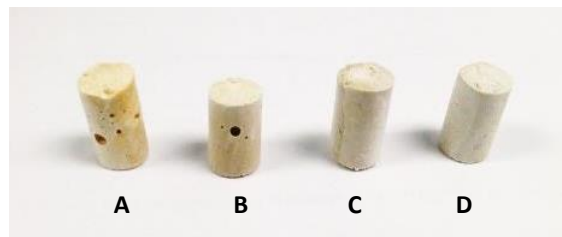
225

226 **3. RESULTS AND DISCUSSION**

227 **3.1. General properties**

228 In general the quality and homogeneity of the samples was found to improve upon the addition of
 229 alginate. Indeed the clay only samples (E) were very friable and crumbled into a powder upon
 230 removal from the vial meaning that suitable monoliths for further tests could not be produced. The
 231 alginate containing samples were much more stable and easier to handle although in some cases
 232 (AC-A, AC-D, PR24-A and PR24-B) visible air voids and defects were observed (FIGURE 1). These
 233 defects appeared to be the result of air-bubbles which are formed during the mixing process in the
 234 higher viscosity samples. This is a similar observation to that made by Gawryla et al. where high
 235 polymer contents and high viscosity mixtures were also found to lead to air entrapment (Gawryla et
 236 al., 2008).

237 **FIGURE 1: Sample Images (PR24)**



238
 239 The bulk density values for all of the samples were found to be within 0.09 – 0.14 g/cm³ range as
 240 shown in TABLE 3. This is within the range of medium density rigid polymer foams (0.08-0.17 g/m³)
 241 (Ashby et al., 2013) but slightly higher than results from Chen et al. (2012) who reported densities of
 242 0.085 g/cm³ for a clay-alginate aerogel with a mix ratio equivalent to the C samples in this study. The
 243 high variability in density, particularly for AC-A, is most likely due to the aforementioned presence of
 244 air voids within the specimens.

245 **TABLE 3: Bulk Density (g/cm³)**

Alg:Clay	A (100:0)	B (75:25)	C (50:50)	D (25:75)
AC	0.12 (±0.03)	0.10 (±0.01)	0.12 (±0.01)	0.10 (±0.01)
PR22	0.13 (±0.02)	0.12 (±0.01)	0.10 (±0.01)	0.09 (±0.01)
PR24	0.10 (±0.01)	0.11 (±0.01)	0.11 (±0.01)	0.11 (±0.01)
PR32	0.11 (±0.01)	0.13 (±0.01)	0.09 (±0.03)	0.11 (±0.01)
PR52	0.11 (±0.01)	0.14 (±0.01)	0.11 (±0.01)	0.09(±0.02)

246

247 **3.2. Mechanical Properties**

248 **3.2.1. Compressive Strength at Yield**

249 Typical stress-strain plots for the aerogels are shown in FIGURE 2 to FIGURE 6, highlighting the
250 variation between specimens incorporating different types of alginate. Most of the samples resulted in
251 a similar profile with an initial linear portion followed by a visible yield point after and a sustained
252 period of elastic strain. In all cases the end of the initial linear phase occurred at low levels of strain
253 which is similar to observations by Nussinovitch et al. (1993).

254

FIGURE 2: Stress-strain plots (AC)

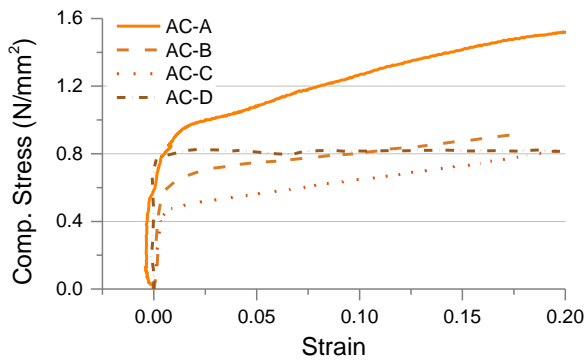


FIGURE 3: Stress-strain plots (PR22)

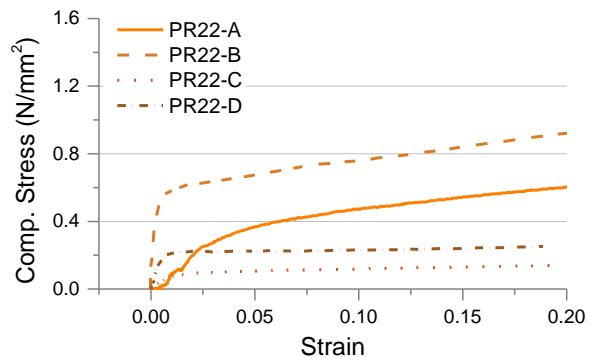


FIGURE 4: Stress-strain plots (PR24)

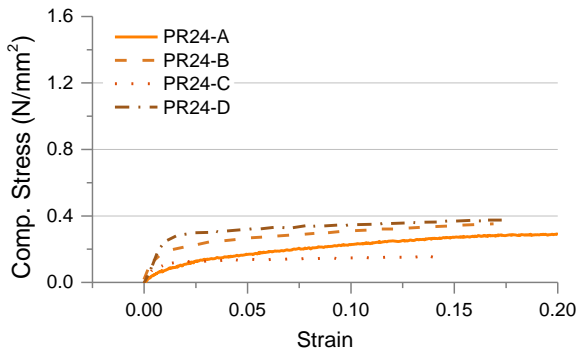


FIGURE 5: Stress-strain plots (PR32)

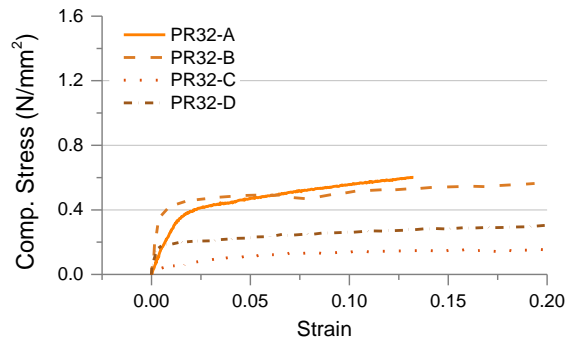
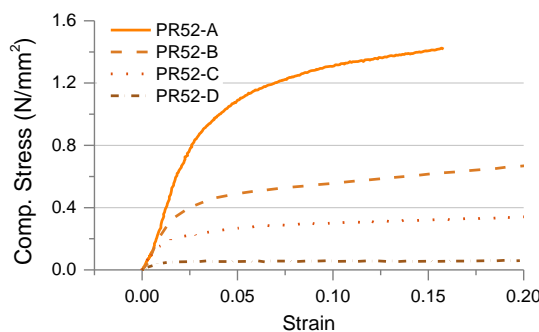


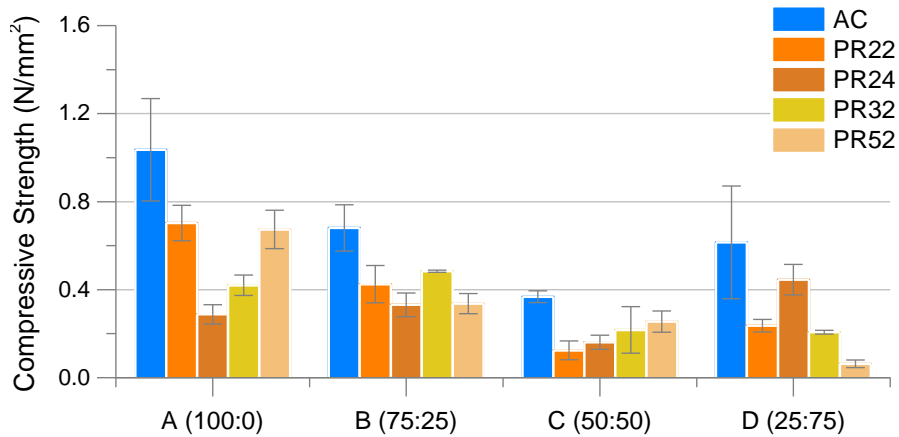
FIGURE 6: Stress-strain plots (PR52)



255

256

FIGURE 7: Compressive Strength



257

258

259 FIGURE 7 demonstrates that the resulting compressive strength values varied quite considerably with
260 results ranging from 0.06 to 1.00 N/mm². Eleven out of the twenty specimens were found to fall within
261 the typical range for low density rigid polymer foams (0.3 – 1.7 N/mm²) (Ashby et al., 2013) with the
262 AC samples appearing to offer the highest strength values. These AC samples provided statistically
263 significant improvements over most of the other alginate types with the exceptions of PR32 and PR52
264 in batch C and PR24 in batch D. The highest strength value was obtained for the alginate only sample
265 and in general strength was found to decrease when the proportion of alginate was replaced with clay
266 down to a ratio of 50:50. Interestingly, the D sample which consisted mainly of the clay with only a
267 25% dosage of alginate, achieved similar results to the 50:50 mix, although the high variability of
268 results should again be noted. PR22 follows a similar pattern to AC with the alginate only sample
269 offering the highest strength whilst lower values were observed for the lower polymer contents. In
270 contrast, PR24 displayed comparatively low strength values for the alginate only sample and the
271 highest value was obtained when only 25% alginate was used. This was most likely due to the fact
272 that the high viscosity PR24 samples resulted in poorer mixing during sample preparation with high
273 polymer contents. This also explains the defects observed in PR24-A and PR24-B. Samples PR32
274 and PR52 exhibited the lowest strength results with the lower polymer dosage and their 75:25 mix
275 ratios offered the most favourable results from the alginate-clay mixes.

276

277 Overall the compressive strength results indicated that whilst the addition of alginate leads to
improvements over the clay control samples, since these samples were too fragile to even be tested,

278 the most effective alginate dosage was dependent upon the specific alginate product used. When
 279 considering ratios B, C and D, for the highest viscosity alginates (ie AC and PR24) an alginate content
 280 of only 25% provided sufficient improvements. However, for the lower viscosity alginates (PR32 and
 281 PR52), better results were achieved with 75% alginate. Furthermore, in terms of alginate
 282 composition, as shown in TABLE 1, PR24 had a much greater G content than the other products
 283 which suggested a greater capacity for crosslinking with calcium. This may explain why PR24
 284 performed better when there was an increased quantity of clay.

285 Although other comparable studies have reported increasing strength values with increasing polymer
 286 content (Ohta and Nakazawa, 1995), this was only visible for some alginate types in our study. The
 287 compressive strength values for the 50:50 mixes were generally lower than for the comparable 50%
 288 starch: 50%clay aerogel (Ohta and Nakazawa, 1995) which achieved a compressive strength value of
 289 0.5 N/mm².

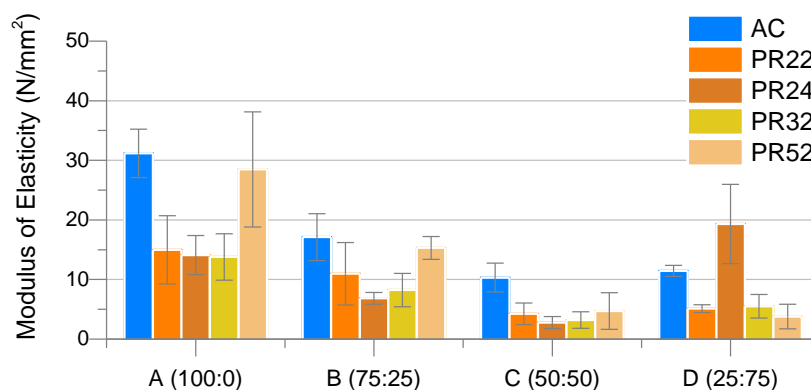
290

291 **3.2.2. Modulus of Elasticity**

292 In comparing the modulus of elasticity values, again results varied depending on the alginate type and
 293 dosage with average values ranging between 3 - 33 N/mm² (FIGURE 8). This was slightly lower than
 294 the range for typical polymer foams (23 – 80 N/mm²) and more comparable to a natural material like
 295 cork (Ashby et al., 2013). However the results for AC-C, PR22-C and PR32-C which fell within the 5 –
 296 10 N/mm² range were similar to the modulus range of 4 – 7 N/mm² reported for PVOH-clay aerogel
 297 (Wang et al., 2013) and that of ~6 N/mm² for a 50:50 alginate-clay aerogel (Chen et al., 2012).

298

FIGURE 8: Modulus of Elasticity



299

300 It should be noted that Chen et al.'s (2012) results also showed a general decrease in modulus values
301 with decreasing alginate content. This trend was apparent for AC, PR22, PR32 and PR52 although
302 slight increases may be observed for the lowest alginate content (D). The exception to this was PR24
303 where the D sample was greater than all of the other mix ratios. Again it is possible in this case that
304 the high viscosity and presence of air voids led to poorer rigidity but this can be improved by
305 increasing the proportion of clay. The particularly high value exhibited by PR24-D compared to the
306 same mix ratio for the other alginate types further highlights the importance of the G content when
307 sufficient quantities of clay are present.

308

309 **3.3. Microstructure**

310 **3.3.1. SEM Analysis**

311 SEM images are displayed in FIGURE 9 to FIGURE 14 at a magnification of 500x. These show the
312 porous structures obtained as a result of the sublimation of the ice crystals. Most of the samples were
313 highly heterogeneous across the fracture surface highlighting that the overall microstructure was not
314 uniform. This can be partly explained by the freezing process since the cell morphology is largely
315 governed by the ice crystal growth which is in turn dependent on the freezing temperature, rate and
316 the direction of heat flow (O'Brien et al., 2004; Wang et al., 2013). In this case whilst the same flash
317 freezing method was adopted for all samples, there was still limited control of the kinetics of ice
318 crystal growth. Therefore although attempts were made to obtain images of the cross-sections of the
319 resulting pores (i.e. perpendicular to the main solidification direction) this could not always be
320 guaranteed. It was therefore difficult to make definitive conclusions from some of the resulting images
321 in terms of quantitative analysis (e.g. mean cell dimensions and cell wall thickness). Nevertheless,
322 some general qualitative observations are offered.

323 In firstly considering, the neat alginate samples (A), the structures are fairly disordered consisting of
324 parallel sheets with relatively thick cell walls. These observations are similar to the irregular
325 topography described by Cheng et al. (2012) for sodium alginate aerogels. However, the pure clay
326 sample (FIGURE 14) displays a distinct lamellar structure, similar to the linear pore structure
327 observed by Nakazawa et al. (1987) for 10 wt% bentonite aerogels. It has been reported that an

328 increase in viscosity can retard ice crystal growth meaning that a higher molecular weight polymer,
329 increased polymer concentration or increased level of cross-linking could increase the likelihood of a
330 cellular, network structure rather than lamellar morphology (Gawryla et al., 2008; Chen et al. 2012).
331 From the images presented here for the composite materials (mix ratios B, C & D), both types of
332 structure are visible.

FIGURE 9: SEM Micrographs - AC

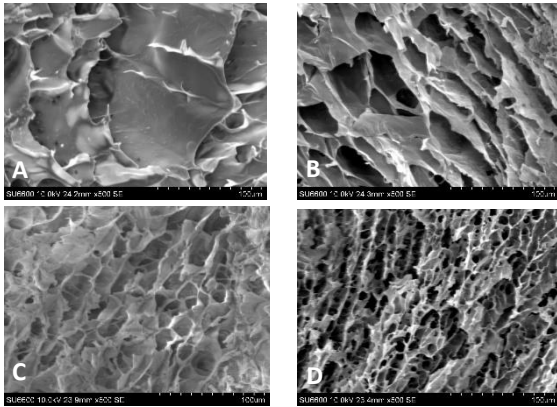


FIGURE 10: SEM Micrographs – PR22

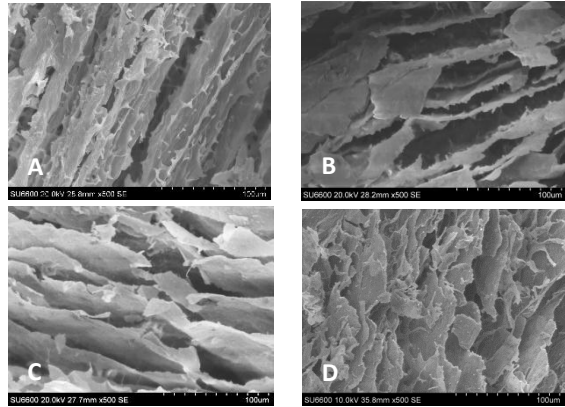


FIGURE 11: SEM Micrographs – PR24

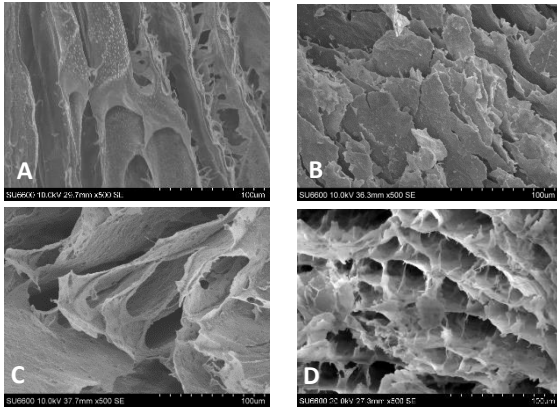


FIGURE 12: SEM Micrographs – PR32

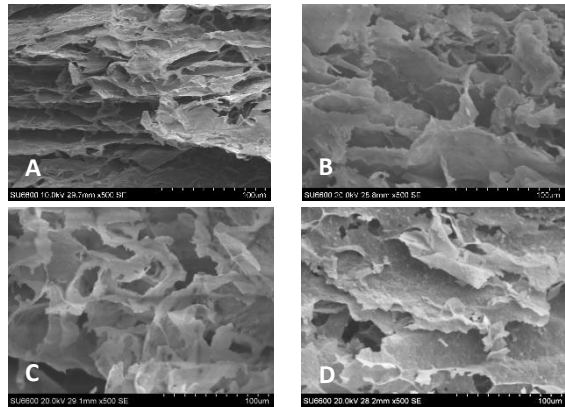


FIGURE 13: SEM Micrographs – PR52

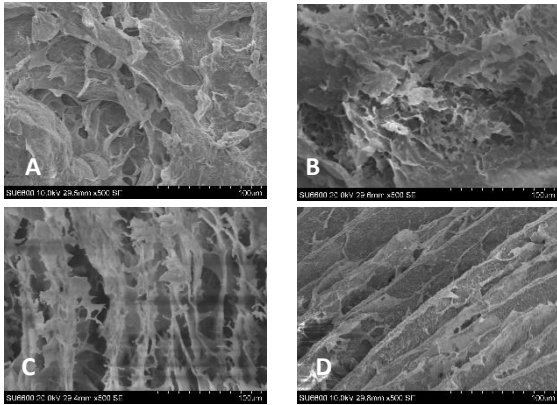
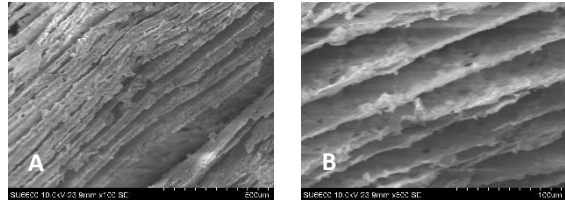


FIGURE 14: SEM Micrographs – Clay (E)



333

334 Relating these observations to the results of the mechanical testing, the formation of a network
335 structure with small cells can help to reduced local stress and can therefore be linked to higher
336 compressive strengths and higher modulus values (Svagan et al., 2011; Wang, 2015). Given that this
337 type of structure is particularly apparent in AC-C, AC-D and PR22-D, this may explain the relatively
338 good strength characteristics of these samples despite their low polymer content. These observations
339 also support work by Chen et al. (2012) where the addition of montmorillonite clay was also found to
340 transform the distinct layered morphology of an alginate aerogel to a co-continuous network which
341 consequently improved the mechanical properties. Gawryla et al. (2008) also described this shift in
342 casein-clay aerogels whereby the separated layers changed to a network structure with the layers
343 connected by a polymer web. This web-like structure reportedly helps to increase the isotropy of the
344 material, meaning that it its less influenced by the size or direction the ice crystal growth.

345 System viscosity can however also have detrimental effect on the aerogel microstructure
346 (Pojanavaraphan et al., 2010). This can lead to the entrapment of air resulting in the formation of
347 spherical voids within the internal structure (Gawryla et al., 2008). For the alginate-clay aerogels (in
348 addition to the macroscopic air bubbles highlighted as part of the visual observations) evidence of
349 these types of defects were also found in the SEM micrographs. It should be acknowledged that the
350 links between the complex variables involved in the ice-templating process and the resulting
351 morphologies, which are in turn linked to the distribution of local stresses and mechanical response,
352 are still not fully understood (Svagan et al., 2011; Li et al., 2012; Deville et al., 2016). However these
353 structural defects clearly have an impact on the structural properties and may explain the high
354 variations in compressive strength and modulus reported.

355

356 **3.3.2. Porosity**

357 Given that the air pores in the aerogel samples are created from the ice crystals formed during
358 freezing, it would be expected that the porosity of the aerogels would be dependent on the volume of
359 water. Since all of the samples are 10 wt% solids, the total theoretical porosity should be close to
360 90%. For the calculated porosities, which are based on the sample weights and volumes, the values
361 range from 93% to 96%. These are close to the values for other polymer-clay aerogels produced
362 using the same solids content. For example Wang (2015) quotes a porosity of around 94% for

363 PVOH-clay aerogels whilst Longo et al. (2013) describe values of close to 90% for PS-clay
 364 composites.

365
 366 **TABLE 4: Estimated Porosity (Alginate Dosage)**

Alg:Clay	AC-A (100:0)	AC-B (75:25)	AC-C (50:50)	AC-D (25:75)	E (0:100)
Bulk Density (g/cm³)	0.097	0.097	0.076	0.104	0.090
Alginate particle density (g/cm³)	1.59	1.1925	0.795	0.3975	0
Clay particle density (g/cm³)	0	0.625	1.25	1.875	2.5
Total Porosity	92.7%	94.6%	94.3%	95.6%	96.4%

367
 368 **TABLE 5: Estimated Porosity (Alginate Type)**

Alg:Clay	AC-C (50:50)	PR22-C (50:50)	PR24-C (50:50)	PR32-C (50:50)	PR52-C (50:50)
Bulk Density (g/cm³)	0.0759	0.0851	0.0349	0.1193	0.1309
Alginate particle density (g/cm³)	0.795	0.795	0.795	0.795	0.795
Clay particle density (g/cm³)	1.25	1.25	1.25	1.25	1.25
Total Porosity	94.3%	95.8%	98.3%	94.2%	93.6%

369 While these high porosity values point towards good thermal performance given the estimated volume
 370 of air, it is acknowledged that a further investigation of the thermal properties would be required in
 371 order to make a clearer comparison with other insulation materials. As previously discussed, thermal
 372 conductivities of 0.02 – 0.4 W/m-K would need to be achieved in order to compete with conventional
 373 materials (e.g. mineral or polymer based products) and values below 0.02 W/m-K would be required
 374 for use in high-performance applications.
 375

376

377 **4.4. Cost and Environmental Impacts**

378 The results from the cost modelling calculations, based on estimated material and production costs
 379 from the aerogel prototypes are presented in TABLE 6. These estimates are based on the purchase
 380 costs and required quantities of the individual materials (from MBL or other suppliers) and calculated
 381 electricity costs based on equipment power consumption and duration of use. The material costs vary
 382 marginally depending upon the mix ratio used and estimated costs include higher costs for clay at
 383 (£20/kg) and slight differences in costs for the *Laminaria Hyperborea* (LH) species (£11/kg) and the
 384 *Acsophyllum Nodosum* (AN) product (£8.50/kg). In terms of production, the greatest cost is
 385 associated with the freeze-drying and the electricity consumed during this process, however these

386 costs are similar to the material costs. In total this gives estimated production costs of approximately
 387 £3 per 100 cm³ sample.

TABLE 6: Cost Estimations

Prototype Samples		£/100cm ³
<i>Materials</i>	Alginate, Clay, Liquid N ₂	£1.62 - £1.69
<i>Processing</i>	Electricity (Mixing & Freeze-drying)	£1.46
<i>Total</i>		£3.08- £3.15

388
 389 These cost calculations are based on laboratory scale equipment however it is acknowledged that for
 390 commercial production, larger and more cost efficient practices would be adopted. Simply
 391 extrapolating the costs of the small samples gives a figure of £308 - £315 per kg or £616 - 630 per m²
 392 assuming that in volumetric terms that the material could be formed into a 20mm thick panel. This of
 393 course excludes other overheads associated with full scale production however still highlights the high
 394 costs involve even in the basic material and drying requirements. For larger scale production, the
 395 main disadvantage is the cost of the liquid nitrogen since the mass of liquid nitrogen required can
 396 equate to more than 3 times the mass of the material being frozen (Smith, 2011). In terms of drying,
 397 again assuming the use of an industrial scale freeze-dryer such as those used within the food
 398 industry, it would be anticipated that cost savings could be achieved compared to the laboratory scale
 399 dryer. Although in comparison with air-drying, the cost of freeze-drying can be 4-8 times more
 400 expensive (Ratti, 2001), there are on-going efforts to increase the efficiency and energy demands of
 401 the freeze-drying process which should help to reduce costs in future (Liu et al., 2008).

402 Furthermore, other studies regarding clay-based aerogels have reported that it is the use of freeze-
 403 drying as an alternative to the relatively expensive solvent exchange and autoclave drying required
 404 for silica aerogels which helps to keep the manufacturing costs low (Schiraldi et al., 2010). Indeed
 405 Dalton et al. (2010) give an estimated cost of £200 per m³ for their clay-polymer product which uses a
 406 similar production process to the aerogels produced in this study. If these production costs could be
 407 achieved, on a m² basis a clay-polymer aerogel would therefore be much less than a silica aerogel
 408 blanket which can cost between £24 - 174/m², depending on product thickness. A recent study in the
 409 UK quoted costs of around £50/m² for a 40mm Spacetherm® product (BRE, 2016) highlighting that
 410 even this composite aerogel product is more than double the cost of a polymer based insulation like

411 PUR and around 7 times greater than mineral wool. All costs must however also be weighed against
 412 the potential long term cost savings in relation to reduced heat losses, and the advantages of
 413 aerogels with regards to the reduced thicknesses required.

414 In considering the environmental analysis of the aerogels, the embodied energy of the alginate, based
 415 on production data from the supplier (MBL) equates to 8.5 and 6.7 MJ/kg of dry alginate product for
 416 the LH and AN products respectively (TABLE 7). It should be noted that these values are lower than
 417 that of the value for 'algae' (20 MJ/kg) used by Galán-Marín et al. (2015) for other composite clay-
 418 alginate materials. This 'algae' data, sourced from Resurreccion et al. (2012), relates to cultivated
 419 micro-algae for biofuel production and therefore requires very different energy and resource inputs to
 420 alginate produced from natural seaweed.

421 Compared to other polymers which are typically used in clay-polymer aerogels such as PVOH which
 422 is used in the aerogels described by Bandi and Schiraldi (2006) and Hostler et al. (2009), it is
 423 reported to have an embodied energy of 60 to 100 MJ per kg (Patel et al., 2003). Other polymers
 424 used in clay aerogels include natural rubber (Pojanavaraphan et al., 2010b) and epoxy resins (Arndt
 425 et al., 2007) which have embodied energy values of 73 MJ/kg and 137 MJ/kg respectively (Hammond
 426 and Jones, 2011). Provided that the rest of the production process were identical, an alginate –based
 427 aerogel would have less of an environmental impact than these other clay-polymer aerogels. For the
 428 clay component, the process for obtaining this material typically involves either hydraulic mining or
 429 open pit extraction followed by purifying, drying, milling, packaging and transport (Heath et al., 2014).
 430 Embodied energy and embodied CO₂ values quoted for bentonite clay, such as those used by Brandt
 431 (2015), are 0.4 MJ/kg and 0.031 kg CO₂/kg. These are not dissimilar to the equivalent values for other
 432 quarried materials like soil, perlite and vermiculite (Hammond and Jones, 2011).

TABLE 7: Embodied Energy (Alginate)

Process		Laminaria Hyperborea MJ/kg	Ascophyllum Nodosum MJ/kg	Laminaria Hyperborea (kg CO _{2e} /kg)	Ascophyllum Nodosum (kg CO _{2e} /kg)
Harvesting	Transport from harvest site to dock	3.10	2.07	0.23	0.16
	Cutting	2.36	1.57	0.18	0.12
Processing (Milling, centrifugation & drying)	Electrical Energy	0.01	0.01	0.00	0.00
	Latent Heat (Fluid Bed Dryer)	0.05	0.05	0.00	0.00
	Sensible Heat	0.02	0.02	0.00	0.00
Water	Washing/ processing	2.93	2.93	0.10	0.10

Total	8.47	6.65	0.51	0.38
--------------	-------------	-------------	-------------	-------------

All energy data based on estimates provided by MBL

433 Aside from the environmental impacts of the materials, the energy requirements associated with the
434 production processes must also be considered. In considering firstly the freezing process, as per the
435 cost modelling, one of the key aspects to consider is the use of liquid nitrogen (N₂) as significant
436 amounts of energy are required in its production. Pušavec et al. (2009) for example quoted a value of
437 1.8 MJ/kg. Water is also used during the production of liquid nitrogen as a cooling fluid, although it is
438 not physically consumed and can therefore be recycled/returned to the environment (Pušavec et al.,
439 2009). Waste outputs are therefore minimal as the cooling water is non-toxic and no CO or SO is
440 produced. According to Ratti (2001), in terms of the overall freeze-drying process, the freezing stage
441 equates to only 4% of the total energy consumption, whilst the sublimation element accounts for
442 around 45%. Overall the energy required to remove 1 kg of water by way of freeze-drying is nearly
443 double of that required using conventional drying methods (Liu et al., 2008). Nonetheless compared
444 to other supercritical drying methods, such as those involving CO₂, it has been argued that freeze-
445 drying offers a more environmentally benign alternative (Schiraldi et al., 2010). There is however
446 currently a lack of evidence to support this statement since a comprehensive LCA for freeze-dried
447 aerogels has yet to be conducted. In fact, according to a recent study regarding drying methods for
448 foodstuffs (Hofland, 2014), supercritical drying with CO₂ was shown to consume less energy than
449 freeze-drying. Lower embodied CO₂ values of 5 kg CO₂ /kg dried product were also reported by
450 Hofland (2014) for the CO₂ methods compared to of 30 kg CO₂ /kg for freeze-drying.

451 Based on the production processes used in this study, estimates regarding the energy inputs for the
452 laboratory scale prototypes are illustrated in TABLE 8. These are also converted to embodied CO₂
453 values in TABLE 9 using the relevant conversion factors (Hill et al., 2013; DECC, 2016). As expected,
454 the greatest energy input is that of the drying phase which constitutes over 90% of the total, meaning
455 that differences between mix ratios are considered minor. The resulting embodied energy estimate of
456 54 MJ per 100cm³ batch of material is similar to the value of 29 MJ per 40cm³ calculated by Dowson
457 et al. (2012) for a high-temperature supercritically dried (HTSD) silica aerogel and lower than that of a
458 low-temperature supercritically dried (LTSD) silica materials (63 MJ per 40cm³ batch). The estimated
459 embodied CO₂ value of 6.2 kg CO₂ per 100cm³ is also higher than that of the HTSD aerogel (0.73 kg
460 CO₂ per 40cm³) but lower than the value of 6.63 kg CO₂ per 40cm³ quoted for the LTSD aerogel.

TABLE 8: Embodied Energy

Materials	Embodied Energy (MJ/kg)	Quantity (kg/ kg)	Total = EE x Quantity (MJ/kg)
Alginate	6.65 – 8.47 ^a	0.25 – 0.75	1.66 – 6.35
Bentonite	0.40 ^b	0.25 – 0.75	0.10 - 0. 03
Liquid Nitrogen	1.80 ^c	100	180
Water	0.01 ^d	9	0.09
Process	Electricity (kWh/kg)	Electricity (MJ/kg)	Total (MJ/kg)
Mixing	18	64.8	64.8
Freeze-drying	1440	5184	5184
Total (MJ/kg)			5395 – 5399
Total (MJ/100 cm³)			54.0

462

a - from Table 7, b –Brandt (2015), c –Pusavec et al. (2010)
d - Hammond and Jones (2011)

TABLE 9: Embodied CO₂

Materials	Embodied CO₂ (kg CO ₂ e / kg)	Quantity (kg/ kg)	Total = EE x Quantity (MJ/kg)
Alginate	0.37 – 0.51 ^a	0.25 – 0.75	0.09 – 0.38
Bentonite	0.03 ^b	0.25 – 0.75	0.01 – 0.02
Liquid Nitrogen	0.21 ^c	100	21
Water	0.001 ^d	9	0.01
Process	Electricity (kWh/kg)	Conversion factor ^e	Total = Electricity x conversion factor (kg CO ₂ e/kg)
Mixing	18	0.41	7.38
Freeze-drying	1440	0.41	590.4
Total (MJ/kg)			618.89 – 619.19
Total (MJ/100 cm³)			6.2

463

464

465

466

a - from Table 7, b – from Ecoinvent (Brandt, 2015), c – Pusavec et al. (2010), d - from Hammond and Jones (2011)
, e – DECC (2016)

467

It should be noted that the calculations for the alginate-clay prototypes are also based on laboratory

468

scale equipment and so energy-efficiency savings would be expected for larger scale production.

469

Indeed Dowson et al. (2012) demonstrated that basic scaling revisions between laboratory scale

470

samples and industrial production involving larger batches could lead to an embodied energy

471

reduction of around two thirds with a similar reduction on the CO₂ burden. If similar savings could be

472

achieved for the clay-aerogel samples, this would give approximate values of below 18 MJ/100 cm³

473

and 2.3 kg CO₂/100cm³. Whilst these are relatively high compared to a commercial silica aerogel

474

blanket (Spacetherm = 0.8 MJ/100 cm³) it should also be noted that the calculation for this product is

475

based on a composite blanket and therefore inclusive of fibres rather than the pure aerogel.

476 Furthermore these estimations are also related to the embodied energy per functional unit rather than
477 the equivalent amount of material required in order to achieve a given U-value. For example, in
478 comparing the thermal performance of different insulators, Dalton et al. (2010) reported that a clay
479 polymer aerogel could be half the thickness of a silica aerogel blanket or a quarter the thickness of
480 and EPC board and achieve an equivalent U-value. Assuming that the thermal conductivity of the
481 alginate-clay aerogel would be similar to that of the clay-polymer aerogels described by Dalton et al.
482 (2010), it is likely that mass of material required would also be less than for conventional insulations.
483 This would have an impact on the overall embodied energy and costs. Further investigation of thermal
484 properties would however be required in order to evaluate the proposed material and compare with
485 the performance of existing products. This would require moving beyond the small scale prototype
486 samples to larger test pieces. As discussed by Alvey et al. (2017) and Lakatos (2017), the impact of
487 moisture conditions and temperature on thermal performance would also need to be considered.

488

489 **5. CONCLUSIONS**

490 In the past decade, high performance insulations such as aerogels have emerged as alternatives to
491 conventional insulating materials and have the potential to reduce heat losses in buildings, particularly
492 in retrofit scenarios where minimum product thicknesses are desirable. Although the high costs of
493 aerogel insulations still hinder their widespread use, strategies to reduce their processing costs and
494 make use of lower cost raw materials, will likely make aerogels more affordable in the future and
495 hence increase the commercial viability of using such materials in bulk applications like building
496 insulation. Furthermore, the use of renewable materials such as biopolymers has been identified as
497 an important strategy in improving the whole life cycle environmental performance and reducing the
498 overall environmental impacts.

499 In this study, clay-alginate aerogels have been investigated as a more environmentally friendly and
500 potentially more economical alternative to existing silica based aerogels. It has been demonstrated
501 that various types of sodium alginate can be added to bentonite clay in order to improve the strength
502 of the aerogels. The small-scale prototypes produced have a low bulk density with mechanical
503 properties similar to other polymer-based foams. It has also been demonstrated that the optimum mix
504 ratio is dependent on the type of alginate used with both polymer viscosity and composition having an

505 effect on potential bonding mechanisms and interactions with the clay. Indeed significant differences
506 in compressive strength, modulus of elasticity and microstructure have been observed in specimens
507 with the same mix proportions and similar bulk densities where the only variable is the alginate
508 source. It is anticipated that further improvements to the mechanical properties could be achieved
509 through the addition of other additives such as an additional calcium source (in order to increase ionic
510 crosslinking potential) and natural fibres (to improve flexural strength and shrinkage) however these
511 measures were out with the scope of the study at this stage.

512 With regards to economic viability, whilst the calculations based on laboratory scale production were
513 found to be high, the majority of costs were associated with freeze-drying element owing to the high
514 cost of liquid N₂ and the electricity consumption required during the drying phase. However, since
515 aerogels are still a developing technology, many of these processing techniques are still being
516 investigated and developed for larger scale production and so it is anticipated that these costs will be
517 reduced with scaling revisions. In terms of the environmental impacts of the material, the embodied
518 energy values for the proposed alginate-clay aerogel are close to the figures reported for silica
519 aerogel monoliths but much higher than that of commercially available silica aerogel blankets. It can
520 therefore not be assumed that the use of natural, renewable materials or freeze-drying methods will
521 guarantee superior environmental performance compared to silica-based aerogels. Given that these
522 comparisons are based on extrapolated values and estimated thermal properties, a more detailed
523 analysis involving the specific thermal conductivity values as well as more accurate production data
524 would shed further light on the environmental performance. A further investigation of the hygrothermal
525 behavior of the samples using larger prototypes would therefore be required in order to fully assess
526 the commercial viability.

527

528 Overall these clay-alginate aerogels have the potential to be used as insulating materials within
529 buildings. Further research into both their specific material properties and appropriate production
530 methods is required however in order to fully assess their technical and commercial viability. Other
531 ongoing work is currently investigating a wider range of alginate types as well as alternatives clays
532 and additional calcium sources. In order to fully assess the suitability of clay-alginate aerogels as a
533 potential insulation material, comparison of other technical properties such as porosity and thermal
534 conductivity is recommended for future research.

536 **ACKNOWLEDGEMENTS**

537 The author wishes to thank the funding providers for the project including the University of
 538 Strathclyde, the Energy Technology Partnership and Marine Biopolymers Ltd. Acknowledgement is
 539 also made to the Advanced Materials Research Lab and the Chemical Processing and Engineering
 540 Department at the University of Strathclyde where the experimental work was conducted.

541 **References**

- 542 Alam, M., Singh, H., Limbachiya, M.C., 2011. Vacuum Insulation Panels (VIPs) for building
 543 construction industry – A review of the contemporary developments and future directions.
 544 Appl. Energy 88, 3592–3602. <https://doi.org/10.1016/j.apenergy.2011.04.040>
- 545 Alvey, J.B., Patel, J., Stephenson, L.D., 2017. Experimental study on the effects of humidity and
 546 temperature on aerogel composite and foam insulations. Energy Build. 144, 358–371.
 547 <https://doi.org/10.1016/j.enbuild.2017.03.070>
- 548 Arndt, E.M., Gawryla, M.D., Schiraldi, D.A., 2007. Elastic, low density epoxy/clay aerogel composites.
 549 J. Mater. Chem. 17, 3525–3529.
- 550 Ashby, M.F., Shercliff, H., Cebon, D., 2013. Materials: engineering, science, processing and design,
 551 3rd ed. Butterworth-Heinemann, Oxford.
- 552 Aspen Aerogels, 2011. Datasheet Spaceloft® High Performance Insulation for Building Envelopes
 553 [WWW Document]. URL http://www.tcnano-norge.no/Spaceloft_10_A2_REV1.pdf (accessed
 554 6.29.15).
- 555 Aspinall, G.O., 2014. The polysaccharides. Academic Press Inc., New York.
- 556 Baetens, R., Jelle, B.P., Gustavsen, A., 2011. Aerogel insulation for building applications: A state-of-
 557 the-art review. Energy Build. 43, 761–769. <https://doi.org/10.1016/j.enbuild.2010.12.012>
- 558 Bandi, S., Schiraldi, D.A., 2006. Glass transition behavior of clay aerogel/poly (vinyl alcohol)
 559 composites. Macromolecules 39, 6537–6545.
- 560 Brandt, A.R., 2015. Embodied Energy and GHG Emissions from Material Use in Conventional and
 561 Unconventional Oil and Gas Operations. Environ. Sci. Technol. 49, 13059–13066.
 562 <https://doi.org/10.1021/acs.est.5b03540>
- 563 BRE, 2016. Rethinking refurbishment: Todmorden and Nelson [WWW Document]. URL
 564 http://www.bre.co.uk/filelibrary/victorian_terrace/pdfs/BRE5776Elevate&Calder-e.pdf
 565 (accessed 6.1.16).
- 566 Buratti, C., Merli, F., Moretti, E., 2017. Aerogel-based materials for building applications: Influence of
 567 granule size on thermal and acoustic performance. Energy Build. 152, 472–482.
 568 <https://doi.org/10.1016/j.enbuild.2017.07.071>
- 569 Carbon Trust, 2012. Building fabric: Energy saving techniques to improve the efficiency of building
 570 structures (No. CTV069).
- 571 Chen, H., Wang, Y., Sánchez-Soto, M., Schiraldi, D., 2012. Low flammability, foam-like materials
 572 based on ammonium alginate and sodium montmorillonite clay. Polymer 53, 5825–5831.
 573 <https://doi.org/http://dx.doi.org/10.1016/j.polymer.2012.10.029>
- 574 Chen, H.-B., Hollinger, E., Wang, Y.-Z., Schiraldi, D.A., 2014. Facile fabrication of poly(vinyl alcohol)
 575 gels and derivative aerogels. Polymer 55, 380–384.
 576 <https://doi.org/10.1016/j.polymer.2013.07.078>
- 577 Cheng, Y., Lu, L., Zhang, W., Shi, J., Cao, Y., 2012. Reinforced low density alginate-based aerogels:
 578 Preparation, hydrophobic modification and characterization. Carbohydr. Polym. 88, 1093–
 579 1099. <https://doi.org/10.1016/j.carbpol.2012.01.075>
- 580 Cuce, E., Cuce, P.M., Wood, C.J., Riffat, S.B., 2014. Toward aerogel based thermal superinsulation
 581 in buildings: A comprehensive review. Renew. Sustain. Energy Rev. 34, 273–299.
- 582 Dalton, J.C., Brase, A., Kuo, N., Marzano, M., 2010. Evacuated Panels Utilizing Clay-Polymer Aerogel
 583 Composites for Improved Housing Insulation. Case Western Reserve University.

584 Davis, T.A., Llanes, F., Volesky, B., Diaz-Pulido, G., McCook, L., Mucci, A., 2003. ¹H-NMR study of
585 Na alginates extracted from *Sargassum* spp. in relation to metal biosorption. *Appl. Biochem.*
586 *Biotechnol.* 110, 75–90.

587 DECC, 2016. UK Government GHG Conversion Factors for Company Reporting.

588 Deville, S., Meille, S., Seuba, J., 2016. A meta-analysis of the mechanical properties of ice-templated
589 ceramics and metals. *Sci. Technol. Adv. Mater.*

590 Dowson, M., Grogan, M., Birks, T., Harrison, D., Craig, S., 2012. Streamlined life cycle assessment of
591 transparent silica aerogel made by supercritical drying. *Appl. Energy* 97, 396–404.

592 Draget, K.I., Skjåk-Bræk, G., Stokke, B.T., 2006. Similarities and differences between alginic acid gels
593 and ionically crosslinked alginate gels. 7th Int. Hydrocoll. Conf. 20, 170–175.
594 <https://doi.org/10.1016/j.foodhyd.2004.03.009>

595 Druel, L., Bardl, R., Vorwerg, W., Budtova, T., 2017. Starch Aerogels: A Member of the Family of
596 Thermal Superinsulating Materials. *Biomacromolecules* 18, 4232–4239.

597 Felton, D., Fuller, R., Crawford, R.H., 2013. The potential for renewable materials to reduce the
598 embodied energy and associated greenhouse gas emissions of medium-rise buildings. *Archit.*
599 *Sci. Rev.* 1–8. <https://doi.org/10.1080/00038628.2013.829022>

600 Finlay, K., Gawryla, M.D., Schiraldi, D.A., 2007. Biologically Based Fiber-Reinforced/Clay Aerogel
601 Composites. *Ind. Eng. Chem. Res.* 47, 615–619. <https://doi.org/10.1021/ie0705406>

602 Funami, T., Fang, Y., Noda, S., Ishihara, S., Nakauma, M., Draget, K.I., Nishinari, K., Phillips, G.O.,
603 2009. Rheological properties of sodium alginate in an aqueous system during gelation in
604 relation to supermolecular structures and Ca²⁺ binding. *Food Hydrocoll.* 23, 1746–1755.
605 <https://doi.org/10.1016/j.foodhyd.2009.02.014>

606 Galán-Marín, C., Rivera-Gómez, C., García-Martínez, A., 2015. Embodied energy of conventional
607 load-bearing walls versus natural stabilized earth blocks. *Energy Build.* 97, 146–154.
608 <https://doi.org/10.1016/j.enbuild.2015.03.054>

609 Gawryla, M.D., Nezamzadeh, M., Schiraldi, D.A., 2008. Foam-like materials produced from abundant
610 natural resources. *Green Chem.* 10, 1078–1081.

611 Grasdalen, H., Larsen, B., Smidsrød, O., 1979. A p.m.r. study of the composition and sequence of
612 uronate residues in alginates. *Carbohydr. Res.* 68, 23–31. [https://doi.org/10.1016/S0008-](https://doi.org/10.1016/S0008-6215(00)84051-3)
613 [6215\(00\)84051-3](https://doi.org/10.1016/S0008-6215(00)84051-3)

614 Hammond, G., Jones, C., 2011. Inventory of Carbon & Energy Version 2.0 (ICE V2. 0). Dep. Mech.
615 Eng. Univ. Bath Bath UK.

616 Heath, A., Paine, K., McManus, M., 2014. Minimising the global warming potential of clay based
617 geopolymers. *J. Clean. Prod.* 78, 75–83.

618 Hill, N., Venfield, H., Dun, C., James, K., 2013. Government GHG conversion factors for company
619 reporting: methodology paper for emission factors. DEFRA DECC.

620 Hofland, G., 2014. Preserving Raw materials Into Excellent and Sustainable End Products While
621 Remaining Fresh (No. 245280).

622 Hostler, S.R., Abramson, A.R., Gawryla, M.D., Bandi, S.A., Schiraldi, D.A., 2009. Thermal conductivity
623 of a clay-based aerogel. *Int. J. Heat Mass Transf.* 52, 665–669.
624 <https://doi.org/10.1016/j.ijheatmasstransfer.2008.07.002>

625 Jelle, B.P., 2011. Traditional, state-of-the-art and future thermal building insulation materials and
626 solutions – Properties, requirements and possibilities. *Energy Build.* 43, 2549–2563.
627 <https://doi.org/10.1016/j.enbuild.2011.05.015>

628 Kiss, B., Manchón, C.G., Neij, L., 2013. The role of policy instruments in supporting the development
629 of mineral wool insulation in Germany, Sweden and the United Kingdom. *Environ. Manag.*
630 *Sustain. Univ. EMSU 2010 Eur. Roundtable Sustain. Consum. Prod. ERSCP 2010* 48, 187–
631 199. <https://doi.org/10.1016/j.jclepro.2012.12.016>

632 Kistler, S.S., 1934. The Relation between Heat Conductivity and Structure in Silica Aerogel. *J. Phys.*
633 *Chem.* 39, 79–86. <https://doi.org/10.1021/j150361a006>

634 Kistler, S.S., 1932. Coherent Expanded Aerogels. *J. Phys. Chem.* 36, 52–64.

635 Kogel, J.E., Trivedi, N.C., Barker, J.M. (Eds.), 2006. Industrial minerals & rocks: commodities,
636 markets, and uses. Society for Mining Metallurgy & Exploration, Colorado, USA.

637 Korjenic, A., Petránek, V., Zach, J., Hroudová, J., 2011. Development and performance evaluation of
638 natural thermal-insulation materials composed of renewable resources. *Energy Build.* 43,
639 2518–2523. <https://doi.org/10.1016/j.enbuild.2011.06.012>

640 Lakatos, Á., 2017. Investigation of the moisture induced degradation of the thermal properties of
641 aerogel blankets: Measurements, calculations, simulations. *Energy Build.* 139, 506–516.
642 <https://doi.org/10.1016/j.enbuild.2017.01.054>

643 Li, W., Lu, K., Walz, J., 2012. Freeze casting of porous materials: review of critical factors in
644 microstructure evolution. *Int. Mater. Rev.* 57, 37–60.

645 Liang, Y., Wu, H., Huang, G., Yang, J., Ding, Y., 2017a. Prediction and Optimization of Thermal
646 Conductivity of Vacuum Insulation Panels with Aerogel Composite Cores. 10th Int. Symp.
647 Heat. Vent. Air Cond. ISHVAC2017 19-22 Oct. 2017 Jinan China 205, 2855–2862.
648 <https://doi.org/10.1016/j.proeng.2017.09.909>

649 Liang, Y., Wu, H., Huang, G., Yang, J., Wang, H., 2017b. Thermal performance and service life of
650 vacuum insulation panels with aerogel composite cores. *Energy Build.* 154, 606–617.
651 <https://doi.org/10.1016/j.enbuild.2017.08.085>

652 Liu, X., Qian, L., Shu, T., Tong, Z., 2003. Rheology characterization of sol–gel transition in aqueous
653 alginate solutions induced by calcium cations through in situ release. *Polymer* 44, 407–412.
654 [https://doi.org/10.1016/S0032-3861\(02\)00771-1](https://doi.org/10.1016/S0032-3861(02)00771-1)

655 Liu, Y., Zhao, Y., Feng, X., 2008. Exergy analysis for a freeze-drying process. *Appl. Therm. Eng.* 28,
656 675–690. <https://doi.org/10.1016/j.applthermaleng.2007.06.004>

657 Lolli, N., Hestnes, A.G., 2014. The influence of different electricity-to-emissions conversion factors on
658 the choice of insulation materials. *Energy Build.* 85, 362–373.
659 <https://doi.org/10.1016/j.enbuild.2014.09.042>

660 Longo, S., Mauro, M., Daniel, C., Galimberti, M., Guerra, G., 2013. Clay exfoliation and polymer/clay
661 aerogels by supercritical carbon dioxide. *Front. Chem.* 1.
662 <https://doi.org/10.3389/fchem.2013.00028>

663 Lopez Hurtado, P., Rouilly, A., Vandenbossche, V., Raynaud, C., 2016. A review on the properties of
664 cellulose fibre insulation. *Build. Environ.* 96, 170–177.
665 <https://doi.org/10.1016/j.buildenv.2015.09.031>

666 Madyan, O.A., Fan, M., Feo, L., Hui, D., 2016. Physical properties of clay aerogel composites: An
667 overview. *Compos. Part B Eng.* 102, 29–37.
668 <https://doi.org/10.1016/j.compositesb.2016.06.057>

669 Martinez, R.G., 2017. Highly Insulated Systems for Energy Retrofitting of Façades on its Interior.
670 *Sustain. Synerg. Build. Urban Scale* 38, 3–10. <https://doi.org/10.1016/j.proenv.2017.03.065>

671 Martins, M., Barros, A.A., Quraishi, S., Gurikov, P., Raman, S.P., Smirnova, I., Duarte, A.R.C., Reis,
672 R.L., 2015. Preparation of macroporous alginate-based aerogels for biomedical applications.
673 *J. Supercrit. Fluids.* <https://doi.org/10.1016/j.supflu.2015.05.010>

674 Martinsen, A., Skjåk-Bræk, G., Smidsrød, O., 1989. Alginate as immobilization material: I. Correlation
675 between chemical and physical properties of alginate gel beads. *Biotechnol. Bioeng.* 33, 79–
676 89.

677 McHugh, D.J., 2003. *A Guide to the Seaweed Industry*. Food and Agriculture Organization of the
678 United Nations, Rome.

679 Nakazawa, H., Yamada, H., Fujita, T., Ito, Y., 1987. Texture control of clay-aerogel through the
680 crystallization process of ice. *Clay Sci.* 6, 269–276.

681 Nosrati, R.H., Berardi, U., 2018. Hygrothermal characteristics of aerogel-enhanced insulating
682 materials under different humidity and temperature conditions. *Energy Build.* 158, 698–711.
683 <https://doi.org/10.1016/j.enbuild.2017.09.079>

684 Nussinovitch, A., Velez-Silvestre, R., Peleg, M., 1993. Compressive characteristics of freeze-dried
685 agar and alginate gel sponges. *Biotechnol. Prog.* 9, 101–104.
686 <https://doi.org/10.1021/bp00019a015>

687 O'Brien, F.J., Harley, B.A., Yannas, I.V., Gibson, L., 2004. Influence of freezing rate on pore structure
688 in freeze-dried collagen-GAG scaffolds. *Biomaterials* 25, 1077–1086.

689 Ohta, S., Nakazawa, H., 1995. Porous clay-organic composites: Potential substitutes for polystyrene
690 foam. *Appl. Clay Sci.* 9, 425–431. [https://doi.org/10.1016/0169-1317\(95\)00003-M](https://doi.org/10.1016/0169-1317(95)00003-M)

691 Papadopoulos, A.M., 2005. State of the art in thermal insulation materials and aims for future
692 developments. *Energy Build.* 37, 77–86. <https://doi.org/10.1016/j.enbuild.2004.05.006>

693 Patel, M., Bastioli, C., Marini, L., Würdinger, E., 2003. Environmental assessment of bio-based
694 polymers and natural fibres. *Life-Cycle Assess. Bio-Based Polym. Nat. Fibres Chapter*
695 “biopolymers 10.

696 Pedroso, M., de Brito, J., Silvestre, J.D., 2017. Characterization of eco-efficient acoustic insulation
697 materials (traditional and innovative). *Constr. Build. Mater.* 140, 221–228.
698 <https://doi.org/10.1016/j.conbuildmat.2017.02.132>

699 Pojanavaraphan, T., Magaraphan, R., Chiou, B.-S., Schiraldi, D.A., 2010a. Development of
700 Biodegradable Foamlike Materials Based on Casein and Sodium Montmorillonite Clay.
701 *Biomacromolecules* 11, 2640–2646. <https://doi.org/10.1021/bm100615a>

702 Pojanavaraphan, T., Schiraldi, D.A., Magaraphan, R., 2010b. Mechanical, rheological, and swelling
703 behavior of natural rubber/montmorillonite aerogels prepared by freeze-drying. *Appl. Clay Sci.*
704 50, 271–279. <https://doi.org/10.1016/j.clay.2010.08.020>

705 Pušavec, F., Stoić, A., Kopač, J., 2009. The role of cryogenics in machining processes. *Teh. Vjesn.*
706 16, 3–9.

707 Rassis, D., Nussinovitch, A., Saguy, I.S., 2003. Tailor-made porous solid foods. *Int. J. Food Sci.*
708 *Technol.* 32, 271–278.

709 Ratti, C., 2001. Hot air and freeze-drying of high-value foods: a review. *J. Food Eng.* 49, 311–319.

710 Rehm, B. (Ed.), 2009. *Alginate: Biology and applications*, Microbiology Monographs. Springer,
711 London.

712 Resurreccion, E.P., Colosi, L.M., White, M.A., Clarens, A.F., 2012. Comparison of algae cultivation
713 methods for bioenergy production using a combined life cycle assessment and life cycle
714 costing approach. *Adv. Biol. Waste Treat. Bioconversion Technol.* 126, 298–306.
715 <https://doi.org/10.1016/j.biortech.2012.09.038>

716 Riffat, S.B., Qiu, G., 2013. A review of state-of-the-art aerogel applications in buildings. *Int. J. Low-*
717 *Carbon Technol.* 8, 1–6.

718 Savio, L., Bosia, D., Patrucco, A., Pennacchio, R., Piccablotto, G., Thiebat, F., 2018. Applications of
719 Building Insulation Products Based on Natural Wool and Hemp Fibers, in: *Advances in*
720 *Natural Fibre Composites*. Springer, pp. 237–247.

721 Scherer, G.W., 1998. Characterization of aerogels. *Adv. Colloid Interface Sci.* 76–77, 321–339.
722 [https://doi.org/10.1016/S0001-8686\(98\)00051-7](https://doi.org/10.1016/S0001-8686(98)00051-7)

723 Schiavoni, S., Bianchi, F., Asdrubali, F., 2016. Insulation materials for the building sector: A review
724 and comparative analysis. *Renew. Sustain. Energy Rev.* 62, 988–1011.

725 Schiraldi, D.A., Bandi, S.A., Gawryla, M.D., 2006. Progress in clay aerogel/polymer composite
726 materials. *Polym. Prepr.* 47, 313.

727 Schiraldi, D.A., Gawryla, M.D., Alhassan, S., 2010. Clay Aerogel Composite Materials. *Adv. Sci.*
728 *Technol.* 63, 147–151.

729 Smith, P.G., 2011. *An Introduction to Food Process Engineering*, 2nd ed, Food Science Text.
730 Springer, USA.

731 Stahl, T., Brunner, S., Zimmermann, M., Ghazi Wakili, K., 2012. Thermo-hygric properties of a newly
732 developed aerogel based insulation rendering for both exterior and interior applications.
733 *Energy Build.* 44, 114–117. <https://doi.org/10.1016/j.enbuild.2011.09.041>

734 Stec, A.A., Hull, T.R., 2011. Assessment of the fire toxicity of building insulation materials. *Energy*
735 *Build.* 43, 498–506. <https://doi.org/10.1016/j.enbuild.2010.10.015>

736 Straatmann, A., Borchard, W., 2003. Phase separation in calcium alginate gels. *Eur. Biophys. J.* 32,
737 412–417.

738 Sutton, A., Black, D., Walker, P., 2011. *Natural Fibre Insulation: An introduction to low-impact building*
739 *materials* (Information Paper No. (IP 18/11)). BRE Ltd.

740 Svagan, A.J., Berglund, L.A., Jensen, P., 2011. Cellulose Nanocomposite Biopolymer Foam:
741 Hierarchical Structure Effects on Energy Absorption. *ACS Appl. Mater. Interfaces* 3, 1411–
742 1417.

743 Thapliyal, P.C., Singh, K., 2014. Aerogels as Promising Thermal Insulating Materials: An Overview. *J.*
744 *Mater.* 2014.

745 Ul Haq, E., Zaidi, S.F.A., Zubair, M., Abdul Karim, M.R., Padmanabhan, S.K., Licciulli, A., 2017.
746 Hydrophobic silica aerogel glass-fibre composite with higher strength and thermal insulation
747 based on methyltrimethoxysilane (MTMS) precursor. *Energy Build.* 151, 494–500.
748 <https://doi.org/10.1016/j.enbuild.2017.07.003>

749 van Olphen, H., 1967. Polyelectrolyte reinforced aerogels of clays - Application as chromatographic
750 absorbents. *Clays Clay Miner.* 15, 423–435. <https://doi.org/10.1346/CCMN.1967.0150142>

751 Wang, L., 2015. *Aerogels based on biodegradable polymers and clay* (PhD Thesis). Universitat
752 Politècnica de Catalunya, Barcelona.

753 Wang, L., Schiraldi, D.A., Sanchez-Soto, M., 2014. Foamlke Xanthan Gum/Clay Aerogel Composites
754 and Tailoring Properties by Blending with Agar. *Ind. Eng. Chem. Res.* 53, 7680–7687.

755 Wang, Y., Gawryla, M.D., Schiraldi, D.A., 2013. Effects of freezing conditions on the morphology and
756 mechanical properties of clay and polymer/clay aerogels. *J. Appl. Polym. Sci.* 129, 1637–
757 1641. <https://doi.org/10.1002/app.39143>

758 Zach, J., Slávik, R., Novák, V., 2016. Investigation of the Process of Heat Transfer in the Structure of
759 Thermal Insulation Materials Based on Natural Fibres. *Ecol. New Build. Mater. Prod.* 2016
760 151, 352–359. <https://doi.org/10.1016/j.proeng.2016.07.389>

761